

Article

Identification of a Cucumber Mosaic Virus from *Cucurbita pepo* on New Reclamation Land in Egypt and the Changes Induced in Pumpkin Plants

Wael Fathy Shehata ^{1,2}, Zafar Iqbal ^{3,*}, Tarek Elsayed Abdelbaset ⁴, Khalied Ibrahiem Saker ⁴, Ahmed Elnabawy El Shorbagy ⁴, Ahmed Mohamed Soliman ⁴, Muhammad Naeem Sattar ³ and Sherif Mohamed El-Ganainy ^{5,6,*}

¹ Department of Agricultural Biotechnology, College of Agriculture and Food Sciences, King Faisal University, Hofuf 31982, Saudi Arabia; wshehata@kfu.edu.sa

² Plant Production Department, College of Environmental Agricultural Science, Arish University, Arish 45511, Egypt

³ Central Laboratories, Hofuf 31982, Saudi Arabia; mnsattar@kfu.edu.sa

⁴ Virus and Phytoplasma Research Department, Plant Pathology Research Institute, Agricultural Research Center, Giza 12619, Egypt; drtarekelsayed71@gmail.com (T.E.A.); khaiedsaker@yahoo.com (K.I.S.); elnabwyahmed@yahoo.com (A.E.E.S.); ahmedsoliman@arc.sci.eg (A.M.S.)

⁵ Department of Arid Land Agriculture, College of Agriculture and Food Sciences, King Faisal University, Hofuf 31982, Saudi Arabia

⁶ Vegetable Diseases Research Department, Plant Pathology Research Institute, Agricultural Research Center (ARC), Giza 12619, Egypt

* Correspondence: zafar@kfu.edu.sa (Z.I.); salganainy@kfu.edu.sa (S.M.E.-G.)



check for updates

Citation: Shehata, W.F.; Iqbal, Z.; Abdelbaset, T.E.; Saker, K.I.; El Shorbagy, A.E.; Soliman, A.M.; Sattar, M.N.; El-Ganainy, S.M. Identification of a Cucumber Mosaic Virus from *Cucurbita pepo* on New Reclamation Land in Egypt and the Changes Induced in Pumpkin Plants. *Sustainability* **2023**, *15*, 9751. <https://doi.org/10.3390/su15129751>

Academic Editors: Antonio Ippolito, Youssef Khamis and Khaled A. El-Tarabily

Received: 4 May 2023

Revised: 14 June 2023

Accepted: 16 June 2023

Published: 19 June 2023



Copyright: © 2023 by the authors. Licensee MDPI, Basel, Switzerland. This article is an open access article distributed under the terms and conditions of the Creative Commons Attribution (CC BY) license (<https://creativecommons.org/licenses/by/4.0/>).

Abstract: In 2020, the leaves and fruit of 50 pumpkin plants with suspected cucumber mosaic virus (CMV) symptoms of leaf mosaic, vein yellowing, and mild leaf curling were collected from Sharq El-Owainat (Al Wadi El-Gaded governorate), a new reclamation land in Egypt. This study was aimed at deciphering and characterizing the causal agent of the leaf yellowing disease associated with pumpkin plants in Egypt. The causal agent was identified by serological, cytological, and molecular means. The serological identification by DAS–ELISA confirmed the presence of CMV in 20% of the plants. The cytological identification by electron microscopy revealed typical cucumovirus isometric particles of 28–30 nm diameter in the cytoplasm of the leaf parenchyma, epidermal cells, the integument, and the nucleus. Molecular characterization by one-step reverse transcriptase-PCR yielded the required size of amplicon (678 bp) for CMV. Additionally, mechanical sap inoculation was used to determine the host range and symptomatology of the isolated CMV in seventeen different plant species belonging to six different plant families. CMV replicated, moved systemically, and induced a range of symptoms in sixteen plant species. The isolated CMV was transmitted to pumpkin plants at a 16.4% rate by seeds. CMV-infected pumpkin plant leaves were characterized by a substantially low concentration of photosynthetic pigments, a high level of reducing sugars, relatively low protein levels, and a significant increase in total phenol contents, implying their potential role as antiviral agents. Ultrathin sections of infected cells revealed histological changes and cytological abnormalities in comparison to healthy plants. This is the first identification of CMV on new reclamation land in Egypt, pinpointing its swift spread, which could pose a major constraint to pumpkin production in Egypt.

Keywords: cucumber mosaic virus (CMV); cucumovirus; DAS–ELISA; electron microscopy; reverse transcriptase PCR; Egypt; cytology

1. Introduction

Pumpkin (*Cucurbita pepo* L.) is an important seasonal crop in the *Cucurbitaceae* family, which also includes gourds, melons, and squash. It is cultivated around the globe with an annual production of 28 million tonnes and is used for different purposes depending on

the region and traditions [1]. In Egypt, pumpkin is harvested on 19,309 hectares, with a total production of 417,109 tonnes [1]. Nowadays, pumpkin is considered an important vegetable due to its nutritional and medicinal properties. It contained considerable amounts of antioxidants, polyphenols, fiber, vitamins (β -carotene, vitamin C, and vitamin E), iron, folate, and several other micro- and macroelements [2]. It can boost immune cells to ward off germs and speed the healing of a wound [3].

Viral infection is a persistent problem in cucurbit commodities, and outbreaks have led to significant yield and quality losses [4]. Cucurbits are known to host ~90 virus species from various families, including *Bromoviridae*, *Closteroviridae*, *Geminiviridae*, *Potyviriidae*, *Solemoviridae*, *Tospoviridae*, and *Virgaviridae* [5,6]. Among these viruses, potyviruses, cucumber mosaic virus (CMV), poleroviruses, and begomoviruses are frequently found associated with cucurbits [5]. In the Mediterranean countries, four viruses, including CMV, watermelon mosaic virus, zucchini yellow mosaic virus (ZYMV), and cucurbit aphid-borne yellow virus (CABYV), are most prevalent [7]. In pumpkin, several viruses, such as pumpkin yellow mosaic virus [8], zucchini yellow mosaic virus [9], papaya ringspot virus [10], squash leaf curl China virus [11], and CMV [12], have been reported.

CMV is a type member of the genus *Cucumovirus* (family *Bromoviridae*) with an icosahedral particle size of 28–30 nm in diameter. It has a single-stranded positive-sense tripartite RNA genome with three genomic RNAs, referred to as RNA1–RNA3, and two subgenomic RNA4 and RNA4A that are encapsidated in a separate icosahedron [13,14]. It has [15] two strains [16] that are divided into two subgroups (referred to as subgroups I and II), based on serological relationships and nucleotide sequence analysis. Subgroup I is further subdivided into IA and IB based on the nucleotide sequence of the 3' UTR of RNA3 [17]. Most strains can be mechanically transmitted *in vitro* to non-host plant species, but naturally, they are transmitted by over 85 species of aphids in a non-persistent manner and by infected seeds [18]. It has been reported to be seed-borne in peas, yardlong beans, and cowpeas (4–18%) [19,20]. It was first discovered on cucumber in 1916 [21], has the most diverse host range compared to any plant virus, and can infect over 1200 plant species belonging to over 100 different plant families. CMV causes a range of symptoms in different plant species, but generally these symptoms include leaf mosaic, yellow discoloration, leaf mottle, vein yellowing, growth stunting, or shoe-stringing [22,23]. It occurs throughout the world in both temperate and tropical climates, affecting a wide range of agricultural and horticultural crops and causing significant economic losses to vegetables and horticultural crops [24]. In Egypt, CMV has been isolated from bananas [25], beans [26], cowpeas [27], tobacco and cucumber [28], and sugar beets [29,30].

Several methods have been employed successfully for detecting and identifying plant viruses, such as ELISA and PCR (immunocapture, reverse transcriptase [RT], multiplex RT-PCR) [31–33]. After introduction into a host plant species, the virus initially conditions the host cell machinery to replicate before spreading to neighboring cells (referred to as cell-to-cell or local movement). Subsequently, the virus enters the vascular tissue and rapidly moves through phloem cells, a phenomenon known as long-distance or systemic movement [34,35]. Plants infected with a virus undergo substantial metabolic and ultrastructural alterations, even when no apparent symptoms are visible [36]. Such metabolic (biochemical) changes may include regulation of different proteins, production of phenolic compounds, assimilation and utilization of carbohydrates, and alteration in chlorophyll contents. All such changes either inhibit or promote disease development or play a significant role in disease resistance [37]. The response of such biochemical compounds in plants has been used as biochemical markers in crop breeding to yield resistant plant genotypes against various biotic and abiotic stresses [38]. The goal of this study was to identify the pathogen responsible for the leaf mosaic, vein yellowing, and mild leaf curling phenotypes in pumpkin plants. In addition, this study was aimed at determining the host range of the pathogen and the ultrastructural changes it caused in pumpkin plants.

2. Materials and Methods

2.1. Sample Collection

On the basis of the phenotypic symptoms of viral disease etiology, leaf samples of pumpkin plants were collected. During the spring of 2020, 2–3 leaf samples and 1–2 fruit samples of 50 different pumpkin plants exhibiting suspected CMV infection symptoms, such as leaf yellowing, mottling, and vein clearing symptoms, were collected from Sharq El-Owainat (22°55'24" N; 28°65'37" E) in Egypt. The collected leaf samples along with fruit were photographed (Figure 1), transported to the lab in polythene bags in a cooler ice box, and stored at -80°C until use.

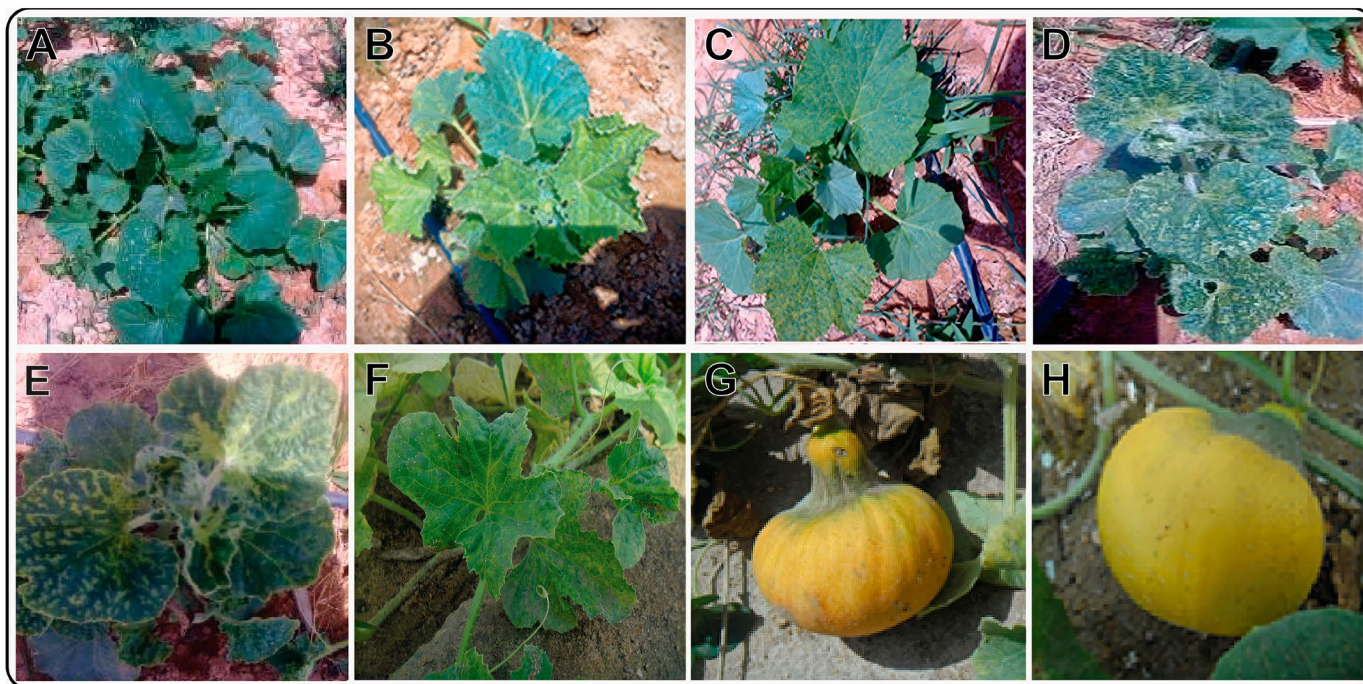


Figure 1. Different phenotypic symptoms observed on pumpkin plants in the Sharq El Owainat region. The collected pumpkin plants showed no symptoms (healthy (A)), edge of the leaf curl (B), yellow spots (C), vein yellowing (clearing) (D,E), and yellow mosaic (F). The infected pumpkin fruits were deformed and small in size (G) compared to healthy fruits (H).

2.2. Serological Assay

A double-antibody sandwich (DAS) enzyme-linked immunosorbent assay (ELISA) was used to detect the virus in pumpkin leaf samples, as described earlier [39], after following the manufacturer's instructions (Bioreba, Switzerland). The collected leaf samples (1 g) were ground in a 5 mL extraction buffer (PBS: 0.13 M NaCl, 0.014 M KH_2PO_4 , 0.08 M Na_2HPO_4 , 0.002 M KCl, pH 7.4, containing 0.05% Tween-20). After coating microplate wells (Nunc Microwell, Denmark) with CMV-specific polyclonal antiserum (in carbonate buffer pH 9.6), the resultant lysate was loaded into the wells. The plates were then incubated at 4°C overnight before being washed three times with PBS/Tween-20 buffer. After washing, plates were coated for 4 h at 37°C with diluted alkaline phosphatase-conjugated antibodies. Following washing with PBS buffer, the wells were loaded with *p*-nitrophenyl phosphate (Sigma Aldrich, St. Louis, MI, USA) in diethanolamine substrate buffer ($0.5\text{ mg}\cdot\text{mL}^{-1}$, pH 9.8) and incubated for 30–180 min at room temperature. The absorbance was measured at 405 nm using a microplate reader (Tecan Spectra II). As negative controls, wells loaded with healthy plant extracts and extraction buffer were used. Only samples whose absorbance values exceeded the mean of the negative controls by at least a factor of three were considered positive, as demonstrated earlier [40].

2.3. Host Range Determination

Seventeen different plant species belonging to six different plant families, including *Amaranthaceae*, *Chenopodiaceae*, *Compositae*, *Cucurbitaceae*, *Leguminosae*, and *Solanaceae*, were obtained from the Agricultural Research Center, Giza, Egypt. All the obtained plant species were grown in a growth chamber at 23 °C with a 16 h light/8 h dark photoperiod cycle. Subsequently, all of these species were used to assess the host range of the virus. The collected pumpkin samples, which tested positive for CMV using DAS–ELISA, were used to prepare inoculum. 1 g of CMV-infected pumpkin leaves were ground in 5 mL of 0.03 M phosphate buffer (pH 7.2). The homogenate was squeezed through a muslin cloth before inoculation. The leaf surface was dusted with carborundum (600 mesh), and then the fully expanded leaves of plants were inoculated at the 2–4 leaf stage. Ten plants of each plant species were sap-inoculated and kept under a conditioned greenhouse until the appearance of typical CMV symptoms. As a control, two plants of each species were mock-inoculated and two were non-inoculated (healthy) and kept separate in the same conditions. After the onset of symptoms, the confirmation of CMV in the systemic leaves of inoculated plant species was achieved by DAS–ELISA, as mentioned above.

2.4. Seed Transmission

To assess the seed transmissibility, five pumpkin plants were mechanically sap inoculated at the 3–5 leaf stage and kept in insect-free cages under greenhouse conditions at 23–25 °C with a 16 h light/8 h dark photoperiod and 80% humidity. As negative controls, non-inoculated (healthy) pumpkin plants were kept separate in insect-free cages under greenhouse conditions. After confirmation of CMV-infected and non-infected (healthy) plants through DAS–ELISA, 55 seeds of CMV-infected plants were collected at maturity and sown in 25 × 30 cm pots containing peat moss, sand, and perlite (1:1:1). The onset of viral symptoms was observed phenotypically after 6 weeks and then confirmed serologically by DAS–ELISA.

2.5. Total RNA Extraction and RT-PCR

Total RNA was extracted from the pumpkin leaves (RNeasy Plant Mini Kit, QIAGEN, Cairo, Egypt), as directed by the manufacturer. A one-step RT-PCR reaction (25 µL volume) was performed using the “iScript One Step qRT-PCR Kit” (BIOMATIK, Kitchener, ON, Canada). Each reaction contained 1 µL of extracted total RNA (40 ng), 12.5 µL of iGreen Mastermix, 1.5 µL (10 µM) of each primer (F4-forward 5'-TTGAGTCGAGTCATGGACAAATC-3' and F3-reverse 5'-AACACGGAATCAGACTGGGAG-3') [41], and 0.5 µL qRT-PCR Enzyme Mix. cDNA was synthesised at 40 °C/30 min and denatured at 94 °C/4 min, followed by 30 cycles of 94 °C/30 s, 45 °C/2 min, 72 °C/2 min, and a final cycle of 72 °C/5 min. Then, 5 µL of the resultant PCR amplicons were resolved on agarose gel (1%) with a DNA marker (100 bp, BIOMATIK, Kitchener, ON, Canada) and photographed using a gel doc system (Syngene Bio Imagins, IN Genius, Cambridge, UK).

2.6. Anatomical and Cytological Studies

A newly emerging terminal leaflet of the fourth leaf (1 cm²) was used for anatomical and cytological studies, as described previously [42]. Plant materials were immediately preserved in a formaldehyde, alcohol, and acetic acid (FAA) solution and dehydrated in a series of ethyl alcohol solutions, from 50% to 100%. The samples were then embedded in paraffin wax (MP 58–61 °C) using xylol as solvent. By using a rotary microtome, 15 micron-thick slices were cut and then mounted on slides with the aid of egg albumin as an adhesive. Wax was dissolved in xylol, and the slides were rehydrated using ethyl alcohol at 100% to 50%. Staining was achieved with safranin and then preserved with Canada balsam as a mounting medium. Finally, plant tissues were visualised under a microscope (Carl Zeiss Jena mounted on a Nikon camera) and photographed.

For the cytological study, infected pumpkin leaf tissues were sliced (1–2 mm), fixed in 2% glutaraldehyde in 0.1 M Na-Cacodylate buffer (pH 7.2), and vacuumed for 1–4 min

after every 15 min for 2 h on ice. Prior to vacuum treatment, floating samples were poked into the buffer and rinsed for 45 min in 0.1 M Na-cacodylate buffer (pH 7.2), with buffer changes every 15 min. The samples were fixed in osmium tetroxide (1%) diluted with Na-cacodylate buffer (pH 7.2) with intermittent vacuum and poking for 1.5 h [43]. After being rinsed in the Na-Cacodylate buffer, the samples were dehydrated in an ethanol series (ranging from 35, 50, 70, 80, 95, and 100%) for 60 min before being infiltrated with the resin. Subsequently, semi-thin sections (1 μm and 90 nm) were prepared on glass slides with the ultra-microtome (Leica model EM-UC6), stained with Toluidine blue for 5 min, and examined by a light microscope (Olympus UC 30 BX 53).

2.6.1. Electron Microscopy

A dip preparation technique was used to photograph the CMV virion under TEM. CMV-infected pumpkin leaf samples and green, nondehydrated, mature seeds were taken, sliced ($\sim 0.5 \text{ mm}^2$), and fixed in modified Karnovsky's fixative (2% glutaraldehyde and 2% paraformaldehyde in 0.05 M cacodylate buffer, pH 7.0) for 2 h at room temperature under low vacuum [44]. After three washings with cacodylate buffer, pumpkin tissues were post-fixed for 2 h in 1% OsO₄ (prepared in cacodylate buffer). Subsequently, tissues were bulk stained overnight with uranyl acetate (0.05%) at 4 °C. The tissues were dehydrated in an ethanol series with propylene oxide before being embedded in Spurr's low-viscosity embedding medium. For electron microscopy, 90 nm thin slices were mounted on 400 mesh copper grids, stained for 10 min with 2% uranyl acetate, then stained for 5 min with lead citrate, and finally examined under a transmission electron microscope (TEM; JEM-1400, JEOL Co., Tokyo, Japan). Electron micrographs were taken using a side-mounted optronics CCD camera (model AMT, 1632 \times 1632 pixels).

2.6.2. Immunogold Labeling

Following fixation in Karnovsky's fixative, the pumpkin tissues were washed twice with cacodylate buffer (0.05 M) for 20 min each, followed by an overnight wash. Tissues were dehydrated in ethanol series (30, 50, and 70%) and then treated with LR White resin (2:1; London Resin Co. Ltd., Basingstoke, UK) in 70% ethanol, followed by an hour-long infiltration in freshly prepared LR White. The tissues were polymerised at 50 °C for 24 h after being embedded in fresh LR White, sliced, subjected to blocking solution (8% nonfat dry milk in PBST; pH 7.3), and incubated for 1 h with anti-CMV polyclonal antibody solution (1:800 in PBST) at room temperature. The sections were washed with PBST buffer before incubation in a dilute solution of anti-rabbit immunoglobulin G-gold conjugate (Sigma; 1:300 in PBST). After thoroughly washing with PBST buffer, the sections were post-stained for 5 min with uranyl acetate (2%) and lead citrate for 2 min, and finally examined under TEM.

2.6.3. Determination of Photosynthetic Pigments

Photosynthetic pigments in pumpkin leaves were measured [45] by grinding 0.2 g of leaf tissue in liquid N₂, then homogenised with 1 mL of N, N-dimethylformamide (DMF; 100%), and centrifuged at 10,000 $\times g$ for 10 min. The supernatant was yielded, and then 1 mL of DMF was added and centrifuged again. The same procedure was repeated. The yielding supernatant was subjected to spectrophotometric measurements at 663 nm and 645 nm. DMF (100%) was used as a blank. Chlorophyll a, b, and total chlorophyll were calculated by the following formulas:

$$\text{Chlorophyll a (mg}\cdot\text{g}^{-1} \text{ tissue)} = [12.7 (\text{OD}_{663}) - 2.69 (\text{OD}_{645})] \times V1000 \times W$$

$$\text{Chlorophyll b (mg}\cdot\text{g}^{-1} \text{ tissue)} = [22.9 (\text{OD}_{645}) - 4.68 (\text{OD}_{663})] \times V1000 \times W.$$

$$\text{Total Chlorophyll (mg}\cdot\text{g}^{-1}\text{ tissue)} = [8.02 (\text{OD}_{663}) + 20.20 (\text{OD}_{645})] \times V1000 \times W.$$

where OD is the optical density at the respective nm, V is the final volume of chlorophyll extract, and W is the fresh weight of the tissues.

2.6.4. Measurement of Total Protein

The total protein content of pumpkin leaves was determined by the Bradford assay [46]. Protein contents were measured in μg of protein per gram of leaf tissue using bovine serum albumin (BSA) as a standard.

2.6.5. Determination of Phenolic Content

The phenolic contents of pumpkin leaves were assessed according to a previously reported method [47]. Fresh pumpkin leaves (250 mg) were ground in 85% methanol, centrifuged at 10 °C for 15 min at 3000 g, and the supernatant was taken. To each 2 mL of the supernatant, 2 mL of Folin–Ciocalteu reagent and 2 mL of sodium carbonate solution (7.5%) were added and incubated for 30–45 min. The absorbance was recorded at 725 nm against a reagent blank. To determine the concentration of total phenols in the samples, a standard curve was created using gallic acid.

2.6.6. Determination of Reducing Sugars

To determine the reducing sugars in the pumpkin samples, the phenol-sulfuric acid method was used [48]. Fresh pumpkin leaf (0.2 g) was ground in deionised water, and the extract was filtered. Then, 2 mL of the extract was mixed with 0.4 mL of phenol (5%). After mixing, 2 mL of 98% H_2SO_4 was quickly added, and tubes were kept at room temperature for 10 min before being incubated at 30 °C for 20 min in a water bath for colour development. Finally, absorbance was recorded at 540 nm against a blank solution, as described earlier [49].

2.7. Assessment of Morphological and Horticultural Attributes

The effect of CMV infection on the morphological and horticultural attributes of pumpkin plants under natural infection was assessed. Ten pumpkin plants, found to harbor CMV, were used to determine their different attributes, such as fruit yield/plant (Kg), fruit weight (g), fruit size (cm^3) by the water displacement method [50], plant height (cm), leaf area (cm^2), and sugar contents. All data were statistically analyzed using Duncan's statistical test.

3. Results

3.1. Phenotype and Serological Assays

A total of 50 pumpkin plant leaves were collected from the reclamation land of Sharq El-Owainat (Al Wadi El-Gaded) governorate in Egypt. The collected pumpkin plants revealed a variety of symptoms as well as a high disease incidence (Figure 1). Nonetheless, some newly emerging leaves were showing curling at the edges of the leaves (Figure 1A). In addition, the fruits of the infected plants were deformed and small in size (Figure 1G).

The results of a serological assay, DAS–ELISA, on 50 pumpkin plants revealed that the incidence of CMV was 20%, with CMV-infected pumpkin plants exhibiting a yellow mosaic and leaf curling phenotype.

3.2. Host Range Studies

Transmission of the isolated CMV was tried on seventeen different plant species belonging to six different plant families through mechanical sap inoculation. All of these plant species were chosen for their (1) experimental nature and (2) cultivation in the area where CMV has been reported. The CMV replicates in sixteen plant species were

successfully inoculated, except *Zinnia elegans* (family *Compositae*), and induced a range of symptoms at 4 to 21 days post-inoculation (Table 1; Figure 2). *Chenopodium quinoa* exhibited chlorotic local lesions at 5 days post-inoculation (dpi), and *C. amaranticolor* showed chlorotic- and necrotic-local lesion phenotypes at 4 dpi (Figure 2D,F). *Piper nigrum* (capsicum) plants exhibited a leaf mosaic phenotype. *Nicotiana tabacum*, *N. benthamiana*, *N. glutinosa*, *Cucumis melo*, and *C. sativus* plants developed mosaic symptoms. The isolated CMV caused necrotic local lesions on *Vigna unguiculata* and *Phaseolus vulgaris* (Figure 2E). Chlorosis of the leaves was observed in *Datura metel* plants at 16 dpi (Figure 2H). A severe leaf crinkle phenotype was induced by CMV on tomato plants at 5 dpi (I). The presence of CMV in the systemic leaves of the inoculated plants was confirmed by DAS-ELISA.

Table 1. Host range and symptoms exhibited by the isolated CMV on different plant species.

Family	Host plant Species (Common Name)	Phenotype *	Incubation Period (Days Post-Inoculation)	Optical Density (405 nm)
Chenopodiaceae	<i>Chenopodium amaranticolor</i> (goosefoot)	CLL NLL	4	+0.423
	<i>C. quinoa</i> (quinoa)	CLL	5	+0.393
	<i>Nicotiana glutinosa</i> (Peruvian tobacco)	SM	15	+0.591
Solanaceae	<i>N. benthamiana</i> (tobacco)	CR MTM	17	+0.734
	<i>N. clevelandii</i> (Cleveland's tobacco)	SCR M	15	+0.531
	<i>Solanum lycopersum</i> (tomato)	LC	05	+0.417
	<i>Datura metel</i> (thorn apple)	Chl	16	+0.484
	<i>Petunia hybrida</i> (petunia)	LM CB	12	+0.611
	<i>N. glauca</i> (tree tobacco)	SLC	15	+0.585
	<i>Solanum melongena</i> (brinjal)	LM	15	+0.743
	<i>Piper nigrum</i> (pepper)	LM	17	+0.708
	Leguminosae	<i>Phaseolus vulgaris</i> (common bean)	SM LP	15
<i>Vigna unguiculata</i> (cowpeas)		NLL	05	+0.611
<i>Vicia faba</i> (broad bean)		VC CH	21	+0.972
Cucurbitaceae	<i>Cucumis sativus</i> (cucumber)	SCR	14	+0.491
Amaranthaceae	<i>Gomphrena globosa</i> (globe amaranth)	Chl	9	+0.235
Compositae	<i>Zinnia elegans</i> (zinnia)	NS	-	-0.083

The values of the controls were also noted at 405 nm; the value of the negative control was 0.105, and the positive control was 0.525. Ten replicates of each plant species were used. * Abbreviations used in the table are the following: CLL, chlorotic local lesions; NLL, necrotic local lesions; SM, systemic mosaic; CR|MTM, chlorotic rings and mottle leaf crinkling; SCR|M, systemic leaf crinkling and mottle; Chl, chlorosis; LM|LB, leaf mosaic and leaf blister; SLC, systemic leaf crinkling; LM, leaf malformation; VC|CH, vein clearing and chlorosis; LC, leaf crinkle; SYM|LP, systemic yellow mosaic and line pattern; and NS, no symptoms.

3.3. Seed Transmission

First-generation seeds obtained from confirmed CMV-infected pumpkin plants were grown and monitored for CMV seed transmission rate. DAS-ELISA results revealed that the seed transmission rate of CMV was 16.3% in pumpkin plants (Table 2). Therefore, these results demonstrate the seed-borne nature of CMV in the pumpkin.

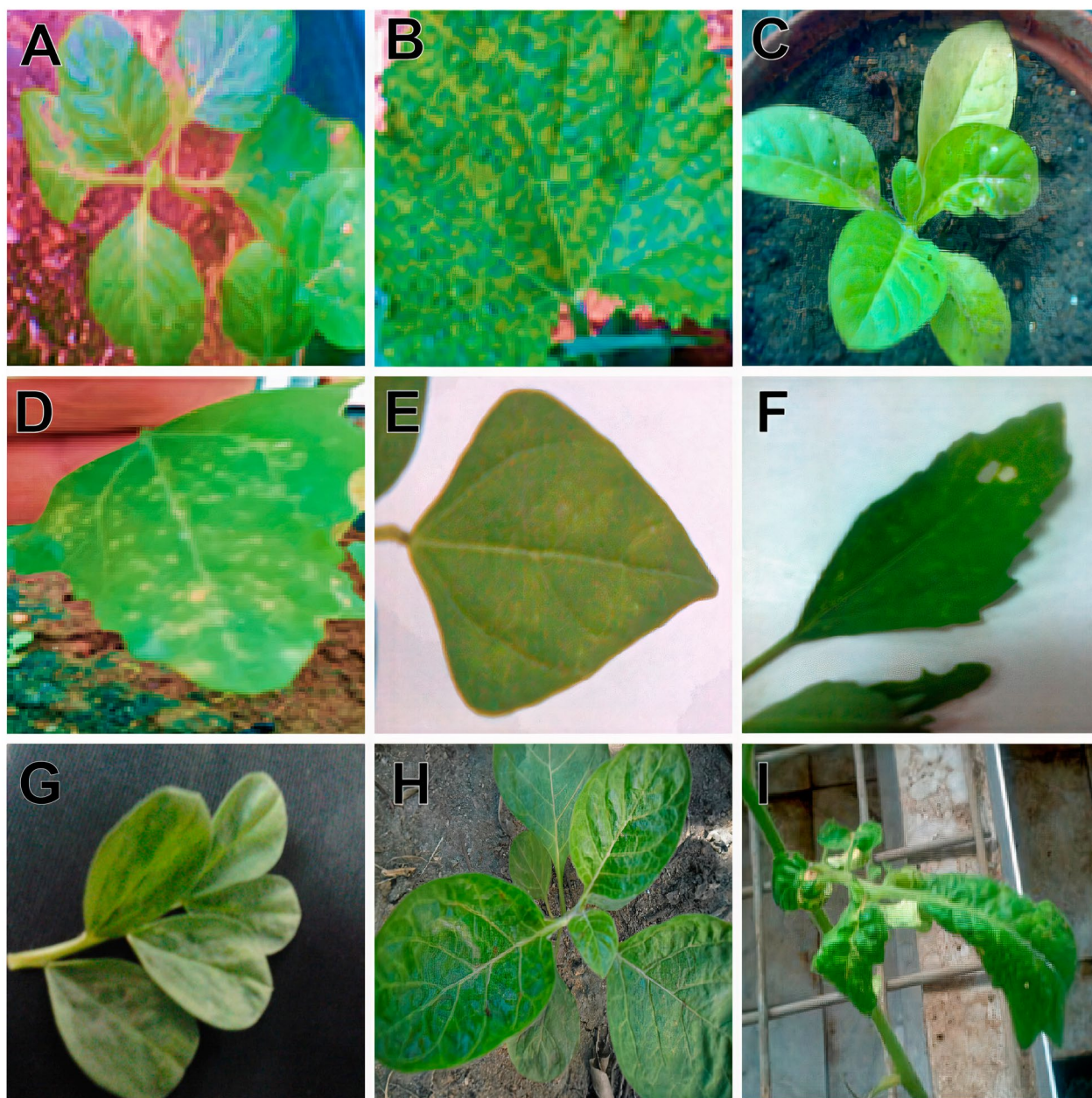


Figure 2. Symptoms induced by the isolated CMV on the systemic leaves of *Nicotiana tabacum* (A), *Cucumis melo* (B), *Nicotiana glutinosa* (C), *Chenopodium amaranticolor* (D), *Phaseolus vulgaris* (E), *Chenopodium quinoa* (F), *Vicia faba* (G), *Datura metel* (H), and *Solanum lycopersicum* (I).

Table 2. Cucumber mosaic virus infection of pumpkin seeds as determined by seed grow-out and DAS-ELISA.

No. of Cultivated Seeds	No. of Seeds without CMV Detection	No. of Seeds With CMV	Transmission%
55	46	9	16.3%

3.4. One-Step RT-PCR

In the pumpkin leaf samples, one-step RT-PCR with a specific set of primers (F3 and F4) for amplification of CMV-encoded coat protein yielded the expected amplicon of ca. 657 kb (Figure 3). All the samples that were found positive with DAS-ELISA showed

successful amplification. No bands were amplified from a healthy leaf obtained from a non-inoculated pumpkin plant, while a positive control, a CMV-coat protein clone, yielded the required amplicon, indicating the specificity of the primers. In PCR, all the necessary negative and positive controls were included.

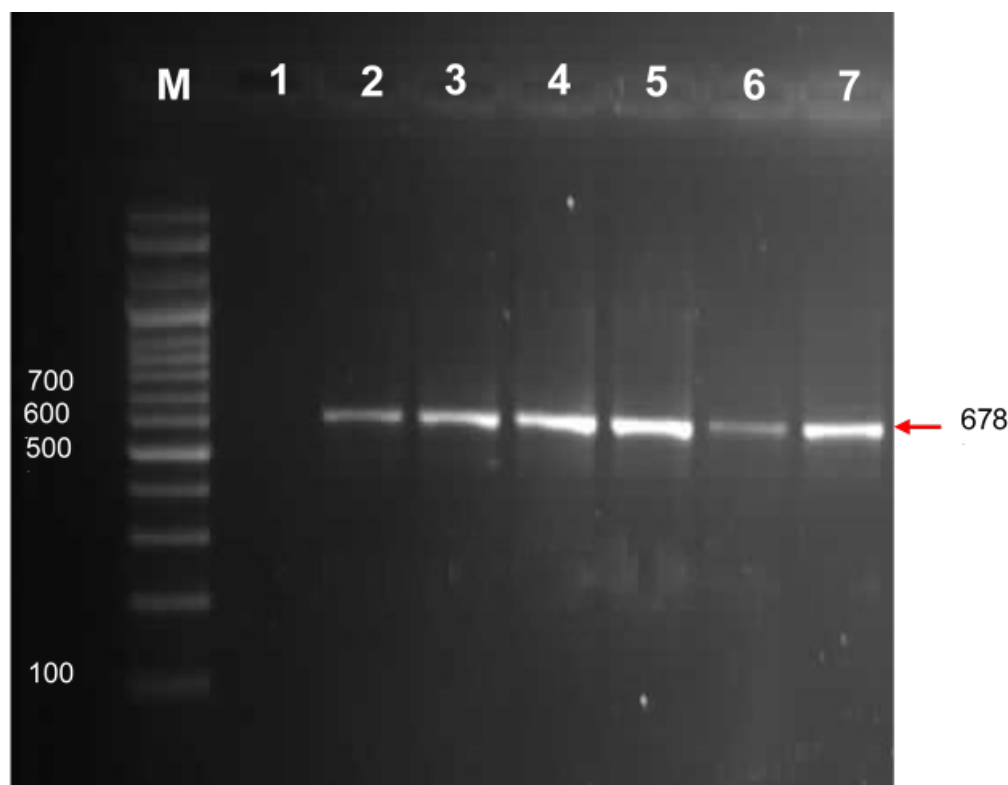


Figure 3. Detection of CMV in pumpkin leaf samples by one-step RT-PCR. A CMV-encoded coat protein gene amplicon of 678 bp was electrophoresed from pumpkin samples (lanes 2–6), a 100 bp DNA marker (BIOMATIK) (lane M), a negative control (healthy plant) (lane 1), and a positive control (lane 7).

3.5. Histological and Cytological Studies

3.5.1. Histological Studies

No intercellular spaces or chloroplasts were observed in the epidermal cells of healthy pumpkin plants. Palisade mesophyll, on the other hand, was found on the adaxial (upper) side of the healthy leaves and contains abundant chlorophyll with a narrow intercellular space between them (Figure 4A). The histological observation revealed that the thickness of the leaflet blade in the infected cells was reduced by 20.64% compared to the healthy plants (Figure 4; Table 3). In contrast, the thickness of the upper and lower epidermal layers increased by 4.15% and 85.48%, respectively. The thickness of palisade and spongy cells increased by 3.25% and 0.42%, respectively. The thickness of the midrib zone was reduced by 29.36%. The length of the protoxylem vessel was shortened by 32.71%, while the length of the metaxylem vessel was increased by 25.63% compared to the control (healthy) plants (Table 3). The cross-sectional center revealed compacted vascular bundles and changes in dimension in the CMV-infected pumpkin plants.

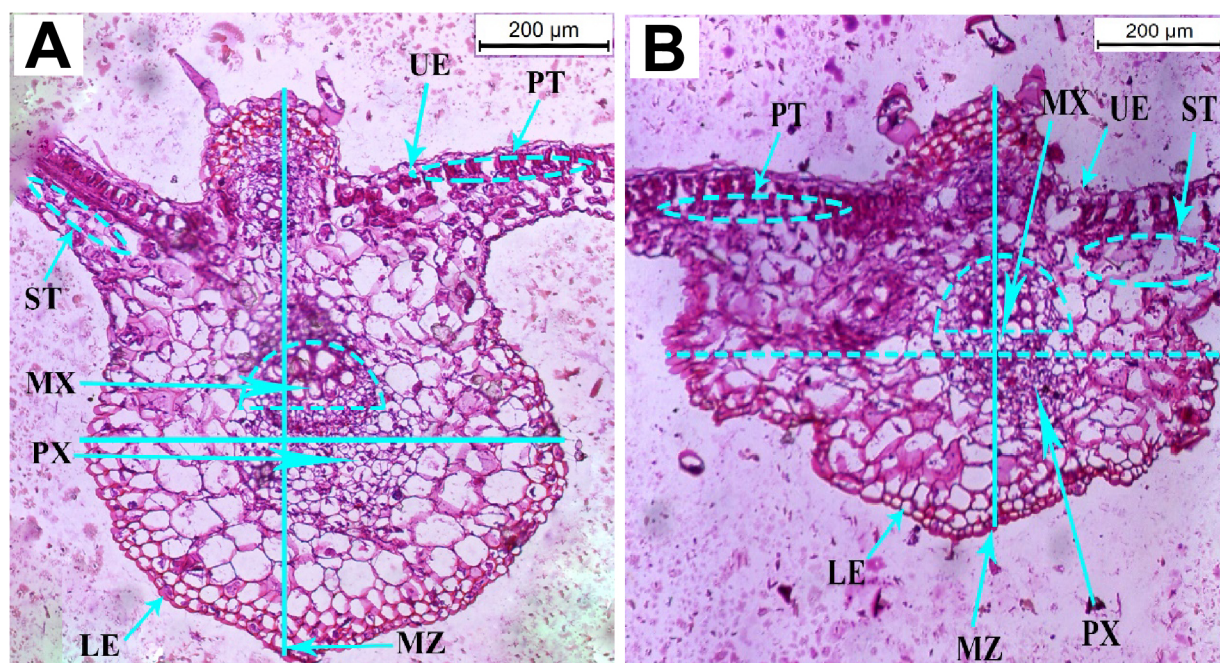


Figure 4. Cross-sections of the anatomical structure of leaflets in healthy (A) and CMV-infected (B) pumpkin plants. Abbreviations used are the following: LB, leaf blade LB; LE, lower epidermal layer; MT, mesophyll tissue; MX, metaxylem; MZ, midrib zone; PT, palisade tissue; PX, protoxylem; ST, spongy tissue; and UE, upper epidermal layer.

Table 3. The anatomical variations observed in the CMV-infected and healthy pumpkin leaves.

Anatomical Attribute	Healthy Plants (μm)	Infected Plants (μm)	% Change
Thickness of the leaflet blade	773.189	613.616	−20.64
Thickness of the upper epidermal layer	17.381	18.102	+4.15
Thickness of the lower epidermal layer	5.278	9.790	+85.48
Thickness of the palisade tissue	28.276	29.196	+3.25
Thickness of the spongy tissue	79.777	80.110	+0.42
Thickness of the midrib zone	837.220	591.427	−29.36
Length of the protoxylem vessel	312.112	210.021	−32.71
Length of the metaxylem vessel	250.100	314.201	+25.63

3.5.2. Cytological Studies

The CMV particles were found in the cytoplasm of leaf parenchyma and epidermal cells, as well as the integument and nucleus cells of pumpkin cells infected with CMV. These virus particles appeared as discrete spheres with diameters of 28–30 nm (Figure 5A).

Electron microscopy comparisons of infected and healthy pumpkin leaf tissues revealed significant differences. An ultrathin section of healthy leaves showed that all the cell organelles and cell wall (CW) were intact and normal in shape (Figure 5B). While

CMV-infected pumpkin plants showed several morphological changes in the organelles. The chloroplasts (Ch) were degraded, had an elongated shape, and contained large starch grains (S) (Figure 5C). The thylakoid membranes were severely damaged, and the grana (G) were reduced in size (Figure 5D,E). The mitochondrion was malformed, aggregated, and had its outer membrane ruptured, implying the effects of virus infection (Figure 5F).

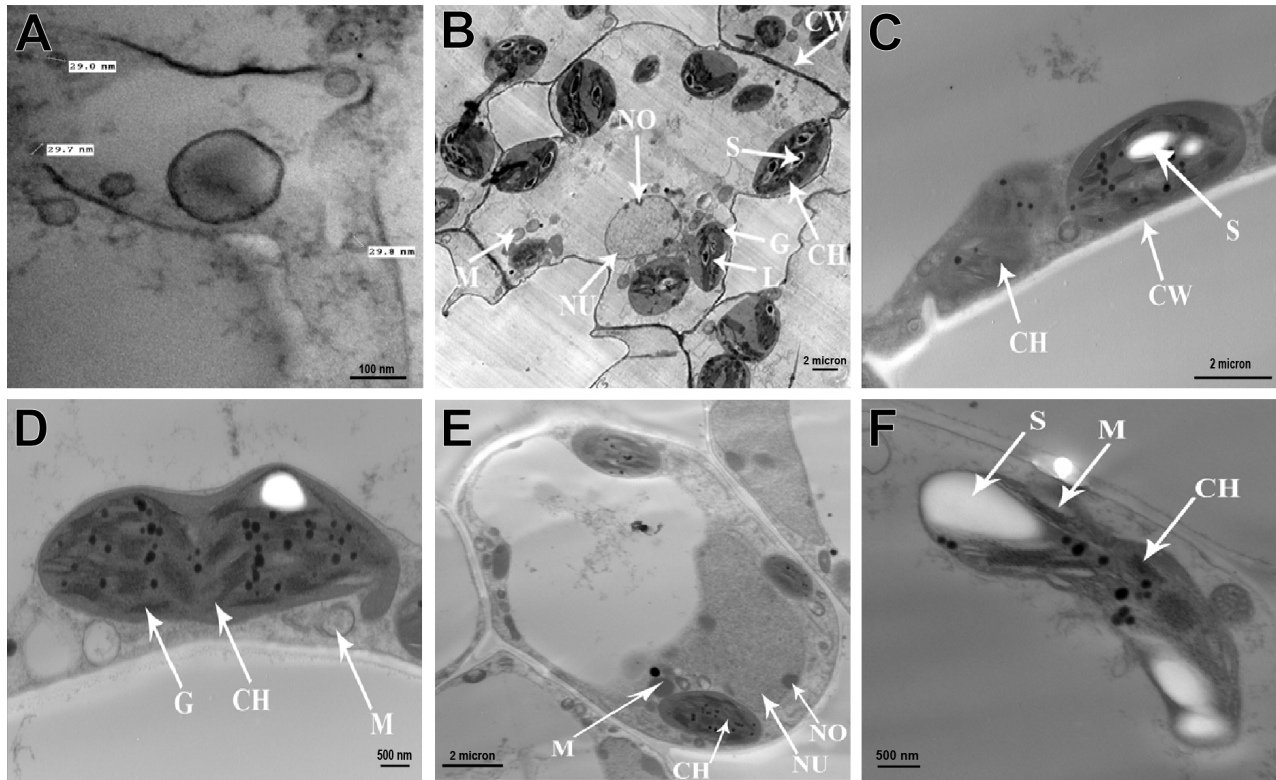


Figure 5. Electron micrographs of CMV-infected pumpkin plant leaf cells. A partial view of the cell shows aggregates of CMV particles in the cytoplasm (A). Ultrathin section of healthy pumpkin leaf cells revealing normal cell wall and normal chloroplast with normal grana and intergrana (B), and infected leaf cells with elongated and de-shaped chloroplasts (C), elongated and aggregated mitochondria (D), elongated nucleus and nucleolus (E), and destructed mitochondria and chloroplasts with large starch grains (F). Abbreviations used in the figure are the following: Nu, nucleus; CH, chloroplast; CW, cell wall; L, intergrana; M, mitochondria; G, grana; S, starch; No, nucleolus.

3.6. Effect of CMV Infection on Biochemical Attributes

CMV-infected pumpkin plants had significantly lower levels of photosynthetic pigments (Figure 6A). Chlorophyll a, chlorophyll b, and total chlorophyll all decreased on average by 33%, 50%, and 38%, respectively.

A significant decrease in foliar protein was observed in CMV-infected pumpkin plants (Figure 6B). This reduction was nearly 35.50% in comparison to healthy plants.

The total phenol contents were higher in CMV-infected pumpkin plants (Figure 6C), and this increase was 33% higher in infected plants than in healthy plants. Reducing sugar levels were almost 10% higher in CMV-infected pumpkin plants than in healthy plants (Figure 6D).

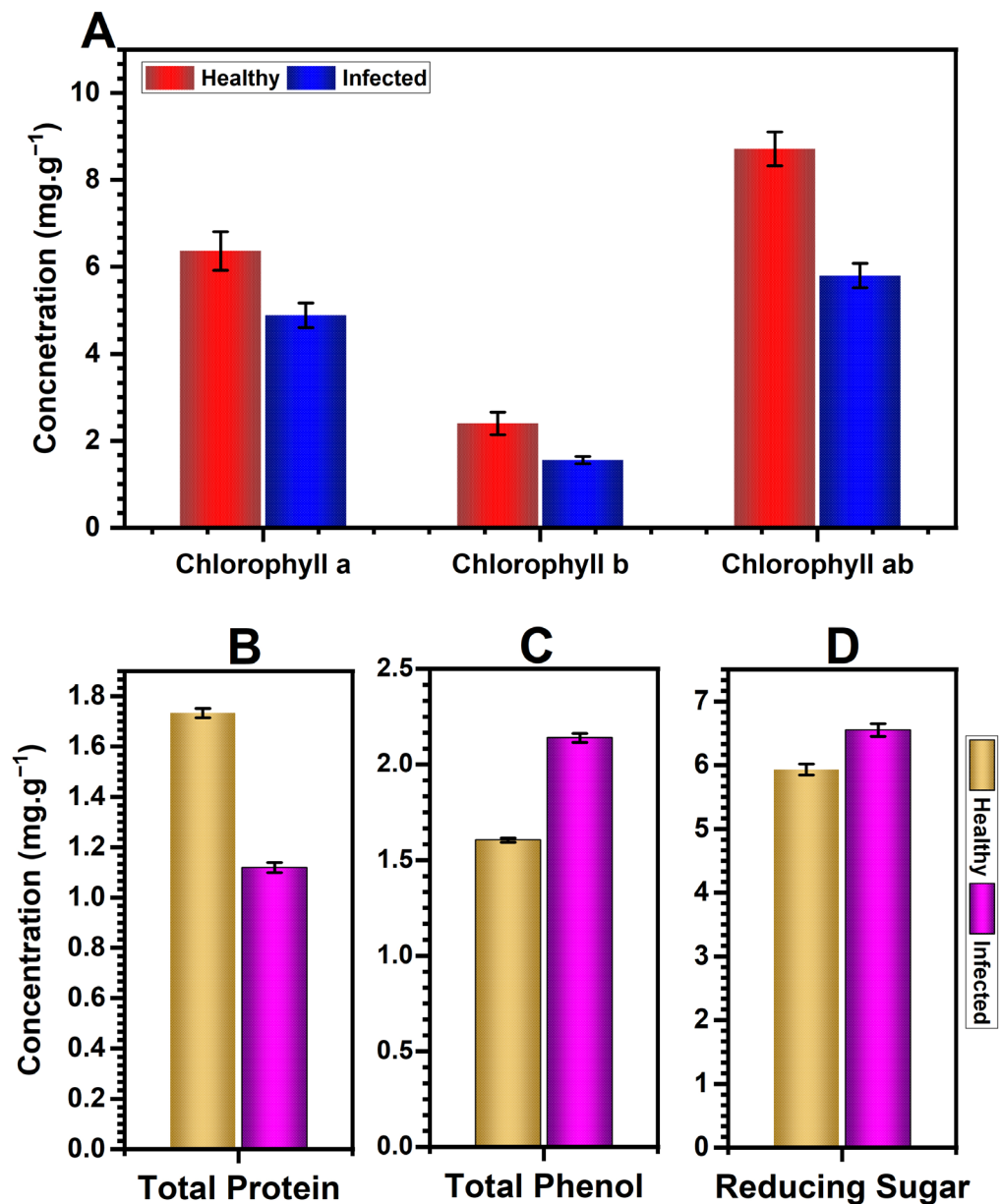


Figure 6. Average photosynthetic pigments, including chlorophyll a, chlorophyll b, and total chlorophyll (A), and average contents of total protein (B), total phenols (C), and reducing sugars (D) of CMV-infected and healthy pumpkin plants. The bar in each column represents the mean of three replicates along with their standard deviation.

3.7. Effects of CMV Infection on Morphological and Horticultural Attributes

CMV infection severely affected the morphological and horticultural attributes of pumpkin plants. Plant height of CMV-infected pumpkin plants was reduced by 22.68%, leaf area was shortened by 44.79%, quantitative yield (the number of fruits) decreased by 41.46%, fruit weight was reduced by 66.07%, and fruit size decreased by 54.20% when compared to healthy plants (Table 4).

Table 4. Effect of CMV on some morphological attributes of infected pumpkin plants.

Name of Attribute	Healthy Plants	CMV-Infected Plants	Relative Change (%)
Plant height (m ²)	3.57 ^a	2.76 ^b	−22.68
Leaf area (cm ²)	98.9	54.6	−44.79
Number of fruits	12.3 ^a	7.2 ^b	−41.46
Fruit Wight (g)	2.8 ^a	0.95 ^b	−66.07
Fruit size (cm ³)	297 ^a	136 ^b	−54.20
Sugar content (mg·g ^{−1})	5.5	3.4	−38.18

All results were calculated at mean values of 10 replicates. Means in the same row with different letters differ significantly ($p < 0.01$).

4. Discussion

CMV is one of the most widespread and destructive phytoviruses, frequently causing significant yield losses in a variety of agro-economically important crops. Diseases caused by CMV have been reported in several crops in Egypt, including bananas, beans, cowpeas, and sugar beets [25,27,30]. Nonetheless, no study is known to decipher the CMV presence in pumpkin plants in Egypt. We may speculate that CMV's introduction to pumpkin plants was a direct transmission from other parts of Egypt or from Sudan, which is nearby. Nonetheless, genome sequencing of already-present CMV in Egypt and Sudan, as well as from pumpkin plants, can reveal information about the genetic lineage of the isolated CMV. The study demonstrated here was designed to investigate the presence of CMV on pumpkin plants on reclaimed land in Egypt.

During the survey, yellow mosaic, mottling, growth stunting, and vein clearing symptoms were observed, while pumpkin fruit displayed reduced size, deformation, and the yellow mosaic phenotype. Previously, similar phenotypes were observed in CMV-infected pumpkin plants [51,52] and pumpkin fruit [53]. Although all the collected pumpkin plants had potential symptoms characteristic of CMV, the CMV incidence determined by DAS-ELISA was merely 20%. Notably, a lower incidence of CMV infection was found on the reclaimed land. The precise reason is unknown, but we can speculate that these symptoms are not always associated with CMV. Other viruses that induce comparable symptoms to CMV are more prevalent in the area, competing for resources with CMV, or the low incidence of CMV may be linked to a low population of insect vectors. All these require further investigations, which can be of interest in futuristic studies. In Illinois, USA, the CMV incidence in pumpkin plants and pumpkin fruits was estimated to be 86% and 11%, respectively. Other studies found 55%, 54%, and 33.33% CMV incidence, respectively, in pumpkin, chillies, and sugar beets [30,54,55]. We found a much lower incidence of CMV, implying a recent introduction of CMV on the reclaimed land of Egypt. However, this speculation needs further investigation. Although all of the plants were collected with symptomatic indicators, such phenotypic indicators are misleading, and visual symptoms must be confirmed by serological detection to obtain accurate information on CMV incidence [55]. A low incidence of the seed transmission rate (16.3%) was demonstrated here, pinpointing that the low incidence of seed transmission in pumpkin plants is most likely due to pumpkin seed compounds (phenolics) that target the viral coat protein N-terminal region of CMV and interfere with proper virion formation and its assembly [56]. Our results corroborated Yang et al. [57], who reported a 15% seed transmission rate of CMV in spinach, and Vitti et al. [56], who reported a 4–16% CMV transmission rate in tobacco seeds. Nonetheless, CMV seed transmission rates were 95–100% in chillies and 57–86% in capsicum [58,59]. Different plant viruses can infect any reproductive tissue, but seed coat and embryo infections are more common. CMV has been identified in all reproductive tissues of spinach [57], only seed coats and embryos of chillies [59], and only in the embryos of tobacco [56]. Notably, the successful seed transmission ability of CMV in pumpkin

seeds may act as a potential inoculum source for its spread, resulting in compromised pumpkin production.

During TEM examinations, spherical particles 28–30 nm in diameter were observed, which is a characteristic feature of CMV as described by [60] and similar to those reported for CMV isolates from sugar beet plants [30,61]. CMV was also identified through molecular characterization of pumpkin plants using a specific primer pair, yielding an amplicon of ca. 678 bp when resolved on gel electrophoresis [30,41].

Depending on the host plant and CMV strain/isolate, CMV induces a wide range of symptoms, including mild to severe yellow mosaic, stunted growth, necrotic or chlorotic lesions, leaf deformation, vein clearing, and shoestring formation [22,23,62–64]. In our study, sixteen of the seventeen plant species inoculated with CMV took up the infection and exhibited a variety of symptoms. Our findings corroborated earlier reports in which CMV induced different phenotypes in different plant species in different parts of the world [21,23,62,65].

Generally, a successful plant virus infection leads to diverse changes in the carbon assimilation, metabolism, structure, development, and growth of the host [66]. Such alterations can range from non-detectable to severe, depending on the severity of the viral strain. In the course of successful infection, a virus must divert host-replication machinery and its biochemical reactions toward its gains; it is reasonable to assume that the virus induces alterations in this communication system. We observed a reduction in the blade thickness of leaflets, an increment in the thickness of the upper and lower epidermal layers, a reduction in the length of the protoxylem vessel, and an increment in the length of the metaxylem vessel. Several studies have investigated the anatomical features of CMV-infected plants and reported the reduction in palisade tissue thickness, mesophyll thickness, and area of both upper and lower epidermis cells from two tomato species and sugar beets [30,67,68], the reduction in the thickness of the xylem zone in the midrib region of the leaf in the infected *Daucus carota* [67], and irregular palisade and spongy cells in papaya and basil [69,70]. The deformation of xylem tissue by CMV in pumpkin plants may be accredited to CMV systemic movement via the xylem, as known for turnip mosaic virus [71]. The biology of virus movement via xylem is currently unknown, owing to the inability to separate vascular components and their pressurized nature.

TEM analysis of CMV-infected pumpkin plant cells revealed chloroplast degradation and elongation, the accumulation of large starch grains, thylakoid membrane damage, and a reduction in the number of grana. These changes suggested that CMV reduced the chloroplast function of the infected plants. The presence of distorted thylakoids and the disappearance of grana stacks suggested that virus pathogenesis uses photosynthesis modification to facilitate infection and virus movement or to establish productive infection or replication within the host [30,72]. The presence of a deformed mitochondrion with a ruptured outer membrane is linked to the disruption of ATP synthesis [73]. All such changes indicate that CMV affects the most important parts of pumpkin cell tissues, resulting in compromised plant forms, structure, and function.

The rate of photosynthetic pigments was found to be significantly lower in our study. The reduction in chlorophyll content in infected pumpkin plants could be attributed to chloroplast disorders, chlorophyll hydrolysis, and/or a loss of leaf photosynthetic area, as witnessed in *Vicia faba* leaves infected with bean mosaic virus [74]. Yellow vein mosaic virus (YVMV) infection resulted in enhanced chlorophyll hydrolysis in okra leaves. YVMV infection further increased the activity of the chlorophyllase enzyme, which is responsible for hydrolyzing chlorophyll, inhibiting chloroplast development, and chlorophyll synthesis [75]. The breakdown of chlorophyll causes mosaic symptoms in infected plants and lowers the photosynthetic rate, and chlorophyll degradation might be used as an indicator of disease severity [76,77]. A reduced photosynthetic rate causes a decrease in the rate of sugar production in the plant, resulting in vigor loss.

In this study, the leaves of CMV-infected pumpkins had significantly higher reducing sugar levels. Our findings are consistent with those of Shalitin and Wolf (2000) [78] and

Shakeel et al. [77], who reported that CMV-infected melon and cucumber leaves had high concentrations of reducing sugars, respectively. Likewise, sunflowers infected with the sunflower chlorotic mottle virus accumulated more sugar [79]. Sugar metabolism is a dynamic process in plant development, and sugar levels and their metabolic fluxes fluctuate significantly throughout plant development and in response to environmental signals, such as biotic and abiotic stresses as well as circadian changes [80,81]. Similarly, potato leafroll virus infection raises sugar levels in tobacco leaves by inhibiting phloem loading [50]. Chillies infected with a mosaic virus had higher levels of reducing sugars [82], and sugarcane leaves infected with the sugarcane yellow leaf virus had higher levels of reducing sugars [83]. The mechanism by which viruses influence phloem loading and sugar accumulation is still unknown. One possible explanation is that plasmodesmata's size-exclusion limit ability has decreased. Furthermore, as viruses typically move systemically via the phloem, potentially blocking sugar movement into the phloem reduces the rate of sugar movement [77,78,84].

Pumpkin plants infected with CMV exhibited an increase in phenolic contents. Corroborating our findings, wheat plants infected with the wheat streak sterility mosaic potyvirus [85] and mungbean plants infected with MYMV [86] had significantly higher phenolic contents than healthy plants. Resistant chilli cultivars infected with the pepper leaf curl virus (PepLCV) [38] and resistant cocoa plants resistant to cocoa swollen shoot virus disease (CSSVD) [87] had been shown to harbor higher phenolic contents. Phenolic compounds are frequently associated with plant responses to various stresses [88]. Rapid phenolic synthesis and polymerization in the cell wall is a potential plant defense response against infection [89,90], whereas low levels of phenolics may be associated with disease susceptibility [91]. In plants, polyphenol oxidase converts phenols to quinone, and phenol accumulation is regulated by phenylalanine ammonia lyase [92].

Protein components have been implicated in plant-pathogen interactions [93,94], with BYDV-susceptible wheat cultivars exhibiting significant protein content reductions [95]. In the current study, pumpkin-infected plants had a significant reduction in protein content. CMV infection has been shown to disrupt protein and carbohydrate levels in the leaves and phloem of infected plants, affecting plant quality for aphid dispersal from infected plants [96].

CMV infection had a significant negative impact on the majority of the pumpkin plant parameters measured in this study, including plant height, leaf area, number, and weight of fruit. All of the investigated attributes showed a substantial reduction, with percentage changes ranging from 22 to 66%. A similar observation has been reported earlier on CMV-infected chilli plants [97]. Nonetheless, the percent effect on these attributes may vary depending on the stage of plant growth at the time of inoculation [98].

5. Conclusions

Conclusively, our results confirmed the presence of CMV in pumpkin plants on reclaimed land in Egypt. Although the incidence of CMV disease was low, indicating a recent introduction, it could become an epidemic in subsequent years if left uncurbed. CMV infection led to significant changes in the biochemical and histological attributes of pumpkin plants, resulting in adverse effects on plant growth and yield. Although the damage to vasculature in CMV-infected plants has yet to be quantified, we may speculate that an accumulating viral load in the phloem leads to more widespread vasculature damage and sugar transport inhibition. Given the importance of pumpkins both as a food and cash crop in Egypt, it is crucial to implement effective measures to prevent and manage CMV infection in pumpkin plants to ensure sustainable crop production.

Author Contributions: Conceptualization, W.F.S. and T.E.A.; methodology, S.M.E.-G., K.I.S., A.E.E.S. and A.M.S.; software, A.M.S. and Z.I.; writing—original draft preparation, W.F.S., T.E.A., K.I.S., A.E.E.S. and M.N.S.; writing—review and editing, Z.I., S.M.E.-G. and A.M.S. All authors have read and agreed to the published version of the manuscript.

Funding: This research was funded by the Deputyship for Research and Innovation, Ministry of Education, in Saudi Arabia, project number INST120.

Institutional Review Board Statement: Not applicable.

Informed Consent Statement: Not applicable.

Data Availability Statement: All the data related to the current study are represented in the manuscript.

Acknowledgments: The authors extend their appreciation to the Deanship of Scientific Research, King Faisal University and all the supporting staff who assisted with this study. Ministry of Education in Saudi Arabia, for funding this research work Deputyship for Research and Innovation, Ministry of Education in Saudi Arabia, for funding this research work (project number INST120).

Conflicts of Interest: The authors declare no conflict of interest.

References

1. FAOStat. Food and Agriculture Organization of the United Nations Statistics Division. Available online: <http://faostat3.fao.org/home/E> (accessed on 25 January 2023).
2. Usha, R.; Lakshmi, M.; Ranjani, M. Nutritional, sensory and physical analysis of pumpkin flour incorporated into weaning mix. *Malays. J. Nutr.* **2010**, *16*, 379–387.
3. Hussain, A.; Kausar, T.; Sehar, S.; Sarwar, A.; Ashraf, A.H.; Jamil, M.A.; Noreen, S.; Rafique, A.; Iftikhar, K.; Aslam, J. Utilization of pumpkin, pumpkin powders, extracts, isolates, purified bioactives and pumpkin based functional food products; a key strategy to improve health in current post COVID 19 period—An updated review. *Appl. Food Res.* **2022**, *2*, 100241. [[CrossRef](#)]
4. Radouane, N.; Ezrari, S.; Belabess, Z.; Tahiri, A.; Tahzima, R.; Massart, S.; Jijakli, H.; Benjelloun, M.; Lahlali, R. Viruses of cucurbit crops: Current status in the Mediterranean Region. *Phytopathol. Mediterr.* **2021**, *60*, 493–519. [[CrossRef](#)]
5. Lecoq, H. Cucurbits. In *Virus and Virus-like Diseases of Major Crops in Developing Countries*; Loebenstein, G., Thottappilly, G., Eds.; Springer: Dordrecht, The Netherlands, 2003; pp. 665–688. [[CrossRef](#)]
6. Desbiez, C. The never-ending story of cucurbits and viruses. *Acta Hort.* **2020**, *1294*, 173–192. [[CrossRef](#)]
7. Lecoq, H.; Desbiez, C. Viruses of cucurbit crops in the Mediterranean region: An ever-changing picture. *Adv. Virus Res.* **2012**, *84*, 67–126.
8. Muniyappa, V.; Maruthi, M.; Babitha, C.; Colvin, J.; Briddon, R.; Rangaswamy, K. Characterisation of pumpkin yellow vein mosaic virus from India. *Ann. Appl. Biol.* **2003**, *142*, 323–331. [[CrossRef](#)]
9. Zechmann, B.; Müller, M.; Zellnig, G. Cytological modifications in zucchini yellow mosaic virus (ZYMV)-infected Styrian pumpkin plants. *Arch. Virol.* **2003**, *148*, 1119–1133. [[CrossRef](#)]
10. Mohammed, H.; Manglli, A.; Zicca, S.; El Hussein, A.; Mohamed, M.; Tomassoli, L. First report of Papaya ringspot virus in pumpkin in Sudan. *New Dis. Rep.* **2012**, *26*, 26–33. [[CrossRef](#)]
11. Ito, T.; Ogawa, T.; Samretwanich, K.; Sharma, P.; Ikegami, M. Yellow leaf curl disease of pumpkin in Thailand is associated with Squash leaf curl China virus. *Plant Pathol.* **2008**, *57*, 766. [[CrossRef](#)]
12. Hamza, E.S.; Al-Naggar, A.; El-Shabrawi, H.; Tolba, I. Characteristics of cucumber mosaic virus isolates infecting cucurbits in Egypt. *Al-Azhar J. Agric. Res.* **2022**, *47*, 172–184. [[CrossRef](#)]
13. Sivakumaran, K.; Bao, Y.; Roossinck, M.J.; Kao, C.C. Recognition of the core RNA promoter for minus-strand RNA synthesis by the replicases of brome mosaic virus and cucumber mosaic virus. *J. Virol.* **2000**, *74*, 10323–10331. [[CrossRef](#)]
14. Sivakumaran, K.; Chen, M.-H.; Roossinck, M.J.; Kao, C.C. Core promoter for initiation of Cucumber mosaic virus subgenomic RNA4A. *Mol. Plant Pathol.* **2002**, *3*, 43–52. [[CrossRef](#)]
15. Palukaitis, P.; Roossinck, M.J.; Dietzgen, R.G.; Francki, R.I. Cucumber mosaic virus. *Adv. Virus Res.* **1992**, *41*, 281–348.
16. García-Arenal, F.; Escriu, F.; Aranda, M.A.; Alonso-Prados, J.L.; Malpica, J.M.; Fraile, A. Molecular epidemiology of Cucumber mosaic virus and its satellite RNA. *Virus Res.* **2000**, *71*, 1–8. [[CrossRef](#)] [[PubMed](#)]
17. Roossinck, M.J. Cucumber mosaic virus, a model for RNA virus evolution. *Mol. Plant Pathol.* **2001**, *2*, 59–63. [[CrossRef](#)]
18. Palukaitis, P.; García-Arenal, F. Cucumoviruses. *Adv. Virus Res.* **2003**, *62*, 241–323. [[PubMed](#)]
19. Gibbs, A.J.; Harrison, B.D. Cucumber mosaic virus. In *Descriptions of Plant Viruses: No. 1. Set 1*; Gibbs, A.J., Harrison, B.D., Murant, A.F., Eds.; Commonwealth Mycological Institute: Kew Surrey, UK, 1970.
20. Abdullahi, I.; Ikotun, T.; Winter, S.; Thottappilly, G.; Atiri, G. Investigation on seed transmission of cucumber mosaic virus in cowpea. *Afr. Crop Sci. J.* **2001**, *9*, 677–684. [[CrossRef](#)]
21. Doolittle, S.P. A new infectious mosaic disease of cucumber. *Phytopathology* **1916**, *6*, 145–147.
22. Green, S.K.; Kim, J. *Characteristics and Control of Viruses Infecting Peppers: A Literature Review*; Asian Vegetable Research and Development Center Shanhua: Tainan, Taiwan, 1991; Volume 18.
23. Zitter, T.; Murphy, J. Cucumber mosaic. *Plant Health Instr.* **2009**, *10*, 2009–051801. [[CrossRef](#)]
24. Mahjabeen; Akhtar, K.P.; Sarwar, N.; Saleem, M.Y.; Asghar, M.; Iqbal, Q.; Jamil, F.F. Effect of cucumber mosaic virus infection on morphology, yield and phenolic contents of tomato. *Arch. Phytopathol. Plant Prot.* **2012**, *45*, 766–782. [[CrossRef](#)]

25. Shalaby, A.A. Molecular detection of an Egyptian isolate of cucumber mosaic virus (CMV) from infected banana using RT-PCR and nucleic acid prob and partial sequence identification. *Egypt. J. Genet. Cytol.* **2002**, *31*, 183–189.
26. Makkouk, K.; Rizkallah, L.; Madkour, M.; El-Sherbeeney, M.; Kumari, S.; Amriti, A.; Solh, M. Survey of faba bean (*Vicia faba* L.) for viruses in Egypt. *Phytopathol. Mediterr.* **1994**, *33*, 207–211.
27. Abd El-Aziz, M. *Studies on Some Viruses Infecting Cowpea Plants*; Alexandria University: Alexandria, Egypt, 2019.
28. Wagih, E.E.; Zalat, M.M.; Kawanna, M.A. Cytological, histological and molecular characterization of two isolates of Cucumber Mosaic Virus (CMV) in Egypt. *Int. J. Phytopathol.* **2021**, *10*, 9–18. [[CrossRef](#)]
29. El-Kady, M.A.S.; Gamal El Din, A.S.; Nakhla, M.K.; Abdel Salam, A.M. A strain of cucumber mosaic virus isolated sugar beet in Egypt. In Proceedings of the 1st National Conference of Pests & Field Crops in Egypt, Ismailia, Egypt, 21–23 October 1985; pp. 617–626.
30. Mokbel, S.; Ahmed, E.; El-Kammar, H.; Kheder, A. Molecular characterization of cucumber mosaic virus and structural changes of infected sugar beet plants. *J. Virol. Sci.* **2020**, *8*, 12–27.
31. Yu, C.; Wu, J.; Zhou, X. Detection and subgrouping of Cucumber mosaic virus isolates by TAS-ELISA and immunocapture RT-PCR. *J. Virol. Methods* **2005**, *123*, 155–161. [[CrossRef](#)] [[PubMed](#)]
32. Chen, S.; Gu, H.; Wang, X.; Chen, J.; Zhu, W. Multiplex RT-PCR detection of *Cucumber mosaic virus* subgroups and *Tobamoviruses* infecting Tomato using 18S rRNA as an internal control. *Acta Biochim. Biophys. Sin.* **2011**, *43*, 465–471. [[CrossRef](#)]
33. Hamdy Abd El-Aziz, M.; Aly Younes, H. Detection of Cucumber mosaic cucumovirus in infected cowpea plants (*Vigna unguiculata* L.) from northern Egypt. *Nov. Res. Microbiol. J.* **2019**, *3*, 326–340. [[CrossRef](#)]
34. Waigmann, E.; Ueki, S.; Trutnyeva, K.; Citovsky, V. The ins and outs of nondestructive cell-to-cell and systemic movement of plant viruses. *Crit. Rev. Plant Sci.* **2004**, *23*, 195–250. [[CrossRef](#)]
35. Hipper, C.; Brault, V.; Ziegler-Graff, V.; Revers, F. Viral and cellular factors involved in phloem transport of plant viruses. *Front. Plant Sci.* **2013**, *4*, 154. [[CrossRef](#)]
36. Yan, S.L.; Lehrer, A.T.; Hajirezaei, M.R.; Springer, A.; Komor, E. Modulation of carbohydrate metabolism and chloroplast structure in sugarcane leaves which were infected by Sugarcane Yellow Leaf Virus (SCYL). *Physiol. Mol. Plant Pathol.* **2008**, *73*, 78–87. [[CrossRef](#)]
37. Ayres, P.G.; Press, M.C.; Spencer-Phillips, P.T. Effects of pathogens and parasitic plants on source-sink relationships. *Photoassimilate Distrib. Plants Crops* **1996**, *8*, 479–499.
38. Lattanzio, V.; Lattanzio, V.M.; Cardinali, A. Role of phenolics in the resistance mechanisms of plants against fungal pathogens and insects. *Phytochem. Adv. Res.* **2006**, *661*, 23–67.
39. Clark, M.F.; Adams, A.N. Characteristics of the microplate method of enzyme-linked immunosorbent assay for the detection of plant viruses. *J. Gen. Virol.* **1977**, *34*, 475–483. [[CrossRef](#)] [[PubMed](#)]
40. Yilmaz, N.K. Interactions between beet necrotic yellow vein virus and beet soilborne virus in different sugar beet cultivars. *Andalou J. Agric. Sci.* **2010**, *25*, 68–74.
41. Lin, H.-X.; Rubio, L.; Smythe, A.B.; Falk, B.W. Molecular population genetics of *Cucumber mosaic virus* in California: Evidence for founder effects and reassortment. *J. Virol.* **2004**, *78*, 6666–6675. [[CrossRef](#)] [[PubMed](#)]
42. Sass, J.E. *Botanical Microtechnique*, 3rd ed.; The Iowa State University Press: Ames, IA, USA, 1958.
43. Osmont, K.; Freeling, M. Characterization of extended auricle (eta) a developmental mutant that affects the blade/sheath boundary in maize. In Proceedings of the Poster from the 43rd Maize Genetics Conference, Lake Geneva, WI, USA, 10–13 March 2005.
44. Kim, K.S.; Fulton, R.W. Ultrastructure of *Datura stramonium* infected with an Euphorbia virus suggestive of a whitefly-transmitted geminivirus. *Phytopathology* **1984**, *74*, 236–241. [[CrossRef](#)]
45. Moran, R.; Porath, D. Chlorophyll determination in intact tissues using N, N-dimethylformamide. *Plant Physiol.* **1980**, *65*, 478–479. [[CrossRef](#)]
46. Bradford, M.M. A rapid and sensitive method for the quantitation of microgram quantities of protein utilizing the principle of protein-dye binding. *Anal. Biochem.* **1976**, *72*, 248–254. [[CrossRef](#)]
47. Singleton, V.L.; Orthofer, R.; Lamuela-Raventós, R.M. Analysis of total phenols and other oxidation substrates and antioxidants by means of folin-ciocalteu reagent. *Methods Enzymol.* **1999**, *299*, 152–178. [[CrossRef](#)]
48. DuBois, M.; Gilles, K.A.; Hamilton, J.K.; Rebers, P.A.; Smith, F. Colorimetric method for determination of sugars and related substances. *Anal. Chem.* **1956**, *28*, 350–356. [[CrossRef](#)]
49. Ammar, E.-D.; Tsai, C.-W.; Whitfield, A.E.; Redinbaugh, M.G.; Hogenhout, S.A. Cellular and molecular aspects of rhabdovirus interactions with insect and plant hosts. *Ann. Rev. Entomol.* **2009**, *54*, 447–468. [[CrossRef](#)]
50. Herbers, K.; Tacke, E.; Hazirezaei, M.; Krause, K.-P.; Melzer, M.; Rohde, W.; Sonnewald, U. Expression of a luteoviral movement protein in transgenic plants leads to carbohydrate accumulation and reduced photosynthetic capacity in source leaves. *Plant J.* **1997**, *12*, 1045–1056. [[CrossRef](#)] [[PubMed](#)]
51. Ruiz-Medrano, R.; Moya, J.H.; Xoconostle-Cázares, B.; Lucas, W.J. Influence of cucumber mosaic virus infection on the mRNA population present in the phloem translocation stream of pumpkin plants. *Funct. Plant Biol.* **2007**, *34*, 292–301. [[CrossRef](#)]
52. Zitikaitė, I.; Staniulis, J.; Urbanavičienė, L.; Žižytė, M. Cucumber mosaic virus identification in pumpkin plants. *Zemdirb.-Agric.* **2011**, *98*, 421–426.

53. Jossey, S.; Babadoost, M. Occurrence and distribution of pumpkin and squash viruses in Illinois. *Plant Dis.* **2008**, *92*, 61–68. [[CrossRef](#)]
54. Svoboda, J.; Leisova-Svobodova, L. First report of squash mosaic virus in ornamental pumpkin in the Czech Republic. *Plant Dis.* **2011**, *95*, 1321. [[CrossRef](#)] [[PubMed](#)]
55. Ashwathappa, K.V.; Krishna Reddy, M.; Venkataravanappa, V.; Madhavi Reddy, K.; Hemachandra Reddy, P.; Lakshminarayana Reddy, C.N. Genome characterization and host range studies of Cucumber mosaic virus belonging to the Subgroup IB infecting chilli in India and screening of chilli genotypes for identification of resistance. *Virus Dis.* **2021**, *32*, 535–547. [[CrossRef](#)]
56. Vitti, A.; Pagán, I.; Bochicchio, B.; De Stradis, A.; Piazzolla, P.; Scopa, A.; Nuzzaci, M. Cucumber mosaic virus is unable to self-assemble in tobacco plants when transmitted by seed. *Plants* **2022**, *11*, 3217. [[CrossRef](#)]
57. Yang, Y.; Kim, K.S.; Anderson, E.J. Seed transmission of cucumber mosaic virus in spinach. *Phytopathology* **1997**, *87*, 924–931. [[CrossRef](#)]
58. Ali, A.; Kobayashi, M. Seed transmission of Cucumber mosaic virus in pepper. *J. Virol. Methods* **2010**, *163*, 234–237. [[CrossRef](#)]
59. Arogundade, O.; Balogun, O.S.; Kumar, P.L. Seed transmissibility of Cucumber mosaic virus in *Capsicum* species. *Int. J. Veg. Sci.* **2019**, *25*, 146–153. [[CrossRef](#)]
60. Francki, R.; Mossop, D.; Hatta, T. Cucumber mosaic virus. No. 213. In *Descriptions of Plant Viruses*; Commonwealth Mycology Institute and Association of Applied Biology: Kew Surrey, UK, 1979.
61. Megahed, A.; El-DougDoug, K.A.; Othman, B.; Lashin, S.; Hassanin, M.; Ibrahim, M.; Sofy, A. Molecular identification and analysis of coat protein gene of Cucumber mosaic cucumovirus sugar beet Egyptian isolate. *Int. J. Plant Pathol.* **2014**, *5*, 70–83. [[CrossRef](#)]
62. Kumari, R.; Bhardwaj, P.; Singh, L.; Zaidi, A.A.; Hallan, V. Biological and molecular characterization of cucumber mosaic virus subgroup II isolate causing severe mosaic in cucumber. *Indian J. Virol.* **2013**, *24*, 27–34. [[CrossRef](#)] [[PubMed](#)]
63. El-DougDoug, K.; Sofy, A.; Hameed, G.; Dawood, R. Intraspecific diversity of Cucumber mosaic Cucumoviridae in Egypt. *Int. J. Virol.* **2014**, *10*, 94–102. [[CrossRef](#)]
64. Pavithra, B.S.; Govin, K.; Renuka, H.M.; Krishnareddy, M.; Jalali, S.; Samuel, D.K.; Himabindu, K. Characterization of cucumber mosaic virus infecting coleus (*Plectranthus barbatus*) in Karnataka. *Virus Dis.* **2019**, *30*, 403–412. [[CrossRef](#)]
65. Rajamanickam, S.; Nakkeeran, S. Molecular characterization of Cucumber mosaic virus infection in chilli (*Capsicum annum* L.) and its phylogenetic analysis. *Int. J. Chem. Stud.* **2020**, *8*, 2967–2970.
66. Berger, S.; Sinha, A.K.; Roitsch, T. Plant physiology meets phytopathology: Plant primary metabolism and plant–pathogen interactions. *J. Exp. Bot.* **2007**, *58*, 4019–4026. [[CrossRef](#)]
67. Afreen, B.; Baghel, G.; Fatma, M.; Usman, M.; Naqvi, Q. Studies on molecular detection of Cucumber mosaic virus and its anatomical and biochemical changes in *Daucus carota* L. *Int. J. Gen. Eng. Biotechnol.* **2010**, *1*, 187–192.
68. Janjić, N.; Erić, Ž. Morphometric and anatomical-histometric characteristics of two varieties of the species *Solanum lycopersicum* L. infected by Cucumber mosaic virus. *Agro. Knowl. J.* **2012**, *13*, 591–602. [[CrossRef](#)]
69. Kunkaliker, S.; Byadgi, A.; Kulkarni, V.; Krishnareddy, M.; Prabhakar, A. Histopathology and histochemistry of papaya ringspot disease in papaya. *Indian J. Virol.* **2007**, *18*, 33–35.
70. El-Attar, A.K.; Mokbel, S.A.; El-Banna, O.-H.M. Molecular characterization of alfalfa mosaic virus and its effect on basil (*Ocimum basilicum*) tissues in Egypt. *J. Virol. Sci.* **2019**, *5*, 97–113.
71. Wan, J.; Cabanillas, D.G.; Zheng, H.; Laliberté, J.-F. Turnip mosaic virus moves systemically through both phloem and xylem as membrane-associated complexes. *Plant Physiol.* **2015**, *167*, 1374–1388. [[CrossRef](#)] [[PubMed](#)]
72. Gunasinghe, U.; Berger, P. Association of potato virus Y gene products with chloroplasts in tobacco. *Mol. Plant. Microbe Interact.* **1991**, *4*, 452–457. [[CrossRef](#)]
73. Song, Z.; Ghochani, M.; McCaffery, J.M.; Frey, T.G.; Chan, D.C. Mitofusins and OPA1 mediate sequential steps in mitochondrial membrane fusion. *Mol. Biol. Cell* **2009**, *20*, 3525–3532. [[CrossRef](#)] [[PubMed](#)]
74. Radwan, D.E.M.; Lu, G.; Fayez, K.A.; Mahmoud, S.Y. Protective action of salicylic acid against bean yellow mosaic virus infection in *Vicia faba* leaves. *J. Plant Physiol.* **2008**, *165*, 845–857. [[CrossRef](#)]
75. Ahmed, N.; Thakur, M.; Bajaj, K. Nature of resistance and effect of yellow vein mosaic virus on moisture, chlorophyll, chlorophyllase and carbohydrate contents of okra. *Veg. Sci.* **1986**, *13*, 339–353.
76. Singh, M.; Singh, J.; Cheema, S. Effect of Cucumber mosaic virus on chlorophyll content and mineral elements in chilli. *Plant Dis. Res.* **1998**, *13*, 125–128.
77. Shakeel, M.; Amer, M.; Al-Saleh, M.; Ashfaq, M.; Haq, M. Changes in chlorophyll, phenols, sugars and mineral contents of cucumber plants infected with cucumber mosaic virus. *J. Phytopathol. Pest Manag.* **2016**, *3*, 1–11.
78. Shalitin, D.; Wolf, S. Cucumber mosaic virus infection affects sugar transport in melon plants. *Plant Physiol.* **2000**, *123*, 597–604. [[CrossRef](#)]
79. Arias, M.C.; Lenardon, S.; Taleisnik, E. Carbon metabolism alterations in sunflower plants infected with the Sunflower chlorotic mottle virus. *J. Phytopathol.* **2003**, *151*, 267–273. [[CrossRef](#)]
80. Borisjuk, L.; Rolletschek, H.; Wobus, U.; Weber, H. Differentiation of legume cotyledons as related to metabolic gradients and assimilate transport into seeds. *J. Exp. Bot.* **2003**, *54*, 503–512. [[CrossRef](#)] [[PubMed](#)]

81. Blasing, O.E.; Gibon, Y.; Gunther, M.; Hohne, M.; Morcuende, R.; Osuna, D.; Thimm, O.; Usadel, B.R.; Scheible, W.-R.D.; Stitt, M. Sugars and circadian regulation make major contributions to the global regulation of diurnal gene expression in *Arabidopsis*. *Plant Cell* **2005**, *17*, 3257–3281. [[CrossRef](#)] [[PubMed](#)]
82. Choudhury, S.; Hu, H.; Larkin, P.; Meinke, H.; Shabala, S.; Ahmed, I.; Zhou, M. Agronomical, biochemical and histological response of resistant and susceptible wheat and barley under BYDV stress. *PeerJ* **2018**, *6*, e4833. [[CrossRef](#)]
83. Gonçalves, M.C.; Vega, J.; Oliveira, J.G.; Gomes, M. Sugarcane yellow leaf virus infection leads to alterations in photosynthetic efficiency and carbohydrate accumulation in sugarcane leaves. *Fitopatol. Bras.* **2005**, *30*, 10–16. [[CrossRef](#)]
84. Shalitin, D.; Wang, Y.; Omid, A.; Gal-On, A.; Wolf, S. Cucumber mosaic virus movement protein affects sugar metabolism and transport in tobacco and melon plants. *Plant Cell Environ.* **2002**, *25*, 989–997. [[CrossRef](#)]
85. Kofalvi, S.; Nassuth, A. Influence of wheat streak mosaic virus infection on phenylpropanoid metabolism and the accumulation of phenolics and lignin in wheat. *Physiol. Mol. Plant Pathol.* **1995**, *47*, 365–377. [[CrossRef](#)]
86. Srivastava, A.; Tiwari, C. Phenolic contents of cucumber as influenced by the infection of Cucumber green mottle mosaic virus (CGMMV). *J. Living World* **1998**, *5*, 1–3.
87. Ofori, A.; Padi, F.K.; Ameyaw, G.A.; Dadzie, A.M.; Lowor, S. Genetic variation among cocoa (*Theobroma cacao* L.) families for resistance to cocoa swollen shoot virus disease in relation to total phenolic content. *Plant Breed.* **2015**, *134*, 477–484. [[CrossRef](#)]
88. Freeman, B.; Beattie, G. An overview of plant defenses against pathogens and herbivores. *Plant Health Instr.* **2008**, *149*, 1–12. [[CrossRef](#)]
89. Matern, U.; Kneusel, R.E. Phenolic compounds in plant disease resistance. *Phytoparasitica* **1988**, *16*, 153–170. [[CrossRef](#)]
90. Sattler, S.; Funnell-Harris, D. Modifying lignin to improve bioenergy feedstocks: Strengthening the barrier against pathogens? *Front. Plant Sci.* **2013**, *4*, 70. [[CrossRef](#)] [[PubMed](#)]
91. Yao, K.; De Luca, V.; Brisson, N. Creation of a metabolic sink for tryptophan alters the phenylpropanoid pathway and the susceptibility of potato to *Phytophthora infestans*. *Plant Cell* **1995**, *7*, 1787–1799. [[CrossRef](#)]
92. Wen, P.-F.; Chen, J.-Y.; Kong, W.-F.; Pan, Q.-H.; Wan, S.-B.; Huang, W.-D. Salicylic acid induced the expression of phenylalanine ammonia-lyase gene in grape berry. *Plant Sci.* **2005**, *169*, 928–934. [[CrossRef](#)]
93. Carvalho, D.d.; Ferreira, R.A.; Oliveira, L.M.d.; Oliveira, A.F.d.; Gemaque, R.C.R. Proteins and isozymes electroforesis in seeds of *Copaifera Langsdorffii* Desf. (*Leguminosae caesalpinioideae*) artificially aged. *Rev. Arvore* **2006**, *30*, 19–24. [[CrossRef](#)]
94. Tornero, P.; Chao, R.A.; Luthin, W.N.; Goff, S.A.; Dangl, J.L. Large-scale structure–function analysis of the Arabidopsis RPM1 disease resistance protein. *Plant Cell* **2002**, *14*, 435–450. [[CrossRef](#)]
95. Xu, L.; Hou, Q.; Zhao, Y.; Ni, Z.; Liang, H.; Liang, R. Biochemical responses of resistant and susceptible wheat cultivars to English grain aphid (*Sitobio avenae* F.) at grain-filling stage. *Acad. J. Biotechnol.* **2016**, *4*, 276–284.
96. Mauck, K.E.; De Moraes, C.M.; Mescher, M.C. Biochemical and physiological mechanisms underlying effects of Cucumber mosaic virus on host-plant traits that mediate transmission by aphid vectors. *Plant Cell Environ.* **2014**, *37*, 1427–1439. [[CrossRef](#)]
97. Rahman, M.S.; Akhter, M.S.; Alam, M.M.; Pervin, N.; Akanda, A.M. Prevalence of Cucumber Mosaic Virus and its impact on growth and yield of different chili cultivar. *Bull. Inst. Trop. Agric. Kyushu Univ.* **2016**, *39*, 65–74. [[CrossRef](#)]
98. Agrios, G.; Walker, M.; Ferro, D. Effect of cucumber mosaic virus inoculation at successive weekly intervals on growth and yield of pepper (*Capsicum annuum*) plants. *Plant Dis.* **1985**, *69*, 52–55. [[CrossRef](#)]

Disclaimer/Publisher’s Note: The statements, opinions and data contained in all publications are solely those of the individual author(s) and contributor(s) and not of MDPI and/or the editor(s). MDPI and/or the editor(s) disclaim responsibility for any injury to people or property resulting from any ideas, methods, instructions or products referred to in the content.